

In-plane optical response of $\text{Bi}_2\text{Sr}_2\text{CuO}_6$

A. A. Tsvetkov

*Material Science Center, Laboratory of Solid State Physics, University of Groningen,
Nijenborgh 4, 9747 AG Groningen, The Netherlands*

and P. N. Lebedev Physical Institute, Russian Academy of Sciences, Leninsky Prospect 53, 117924 Moscow, Russia

J. Schützmann

*Material Science Center, Laboratory of Solid State Physics, University of Groningen,
Nijenborgh 4, 9747 AG Groningen, The Netherlands*

J. I. Gorina and G. A. Kaljushnaia

P. N. Lebedev Physical Institute, Russian Academy of Sciences, Leninsky Prospect 53, 117924 Moscow, Russia

D. van der Marel

*Material Science Center, Laboratory of Solid State Physics, University of Groningen,
Nijenborgh 4, 9747 AG Groningen, The Netherlands*

(Received 27 August 1996; revised manuscript received 23 December 1996)

We report on infrared reflectivity measurements of the *ab*-plane response of superconducting $\text{Bi}_2\text{Sr}_2\text{CuO}_6$ single crystals. The frequency-dependent conductivity has a maximum near 500 cm^{-1} at room temperature, which shifts to lower frequency and merges with a Drude peak below 100 K. We attribute the unusual behavior of the midinfrared conductivity to low-frequency transitions between electronic bands of mainly BiO character near the \bar{M} point. The linear temperature dependence of the low-frequency resistivity can be followed down to approximately 40 K where it saturates. [S0163-1829(97)01522-1]

The relatively simple crystal structure of single-layer compounds offers the possibility to study intrinsic properties of the CuO_2 plane. It is, however, not clear to what extent the BiO layers contribute to the optical conductivity and how the hole doping into the CuO_2 -planes proceeds. Previously, it was suggested from an optical study of $\text{Tl}_2\text{Ba}_2\text{CaCu}_2\text{O}_8$ that the TlO layers exhibit nonconducting behavior.¹ The situation for the $\text{Bi}_2\text{Sr}_2\text{CuO}_6$ system might be more complex. Band structure calculations using the generalized potential augmented plane-wave (LAPW) method by Singh and Pickett² show that weak structural distortions shift the BiO(3)-derived bands below the Fermi level.

Since the normal-state dynamics is of special interest for understanding strongly correlated electron systems, the low T_c ($< 10\text{ K}$) of the single-layer $\text{Bi}_2\text{Sr}_2\text{CuO}_6$ compound offers the opportunity to examine these features well below the transition temperature of the related double- and triple-layer systems. It is widely accepted that the in-plane response of the cuprates is in the clean limit and the strong midinfrared response is due to strong correlation effects in the cuprates. In particular the marginal Fermi-liquid³ (MFL) and Luttinger-liquid⁴ approaches along with the conventional strong electron-phonon interaction⁵ have been put forward to account for these unusual properties. In these models the strong midinfrared (MIR) conductivity is related to the linear frequency dependence of the scattering rate of the quasiparticles in a single-band picture. Therefore, the normal-state properties of the in-plane conductivity of $\text{Bi}_2\text{Sr}_2\text{CuO}_6$ down to approximately 10 K should play a pivotal role in a clear separation of the different excitations.

In this paper we report on the far-infrared (FIR) *ab*-plane conductivity of a $\text{Bi}_2\text{Sr}_2\text{CuO}_6$ single crystal that was calculated via a Kramers-Kronig analysis of the measured reflectivity data. Above 70 K the conductivity increases with frequency until it reaches a maximum, the frequency of which increases with increasing temperature. The temperature dependence of the low-frequency conductivity is consistent with the dc resistivity measured on crystals of the same batch. Based on the f sum rule we argue that phonon contributions are too weak to account for this maximum. We discuss a scenario where the unusual temperature dependence is due to intraband and interband transitions within and between electronic bands near E_F of CuO_2 and BiO character.

$\text{Bi}_2\text{Sr}_2\text{CuO}_6$ single crystals were grown from a precursor dissolved in liquid KCl.⁶ Due to the formation of an enclosed cavity of a few cm^3 within the melt, samples were obtained as free-standing crystalline platelets of sizes up to $1-2 \times 1-2\text{ mm}^2$ and of thickness $5-20\text{ }\mu\text{m}$.⁷ A constant cavity temperature of $840-850\text{ }^\circ\text{C}$ and a constant temperature gradient ($2-3\text{ K/cm}$) were kept within the melt in order to provide permanent transport of the precursor to the growth zone, which is important for a free growth of homogeneous crystals with a flat mirror surface. Such samples require no mechanical or chemical polishing prior to the infrared reflectivity measurements. X-ray measurements revealed a perfect crystal structure with lattice parameters $a = 5.36\text{ }\text{Å}$, $b = 5.37\text{ }\text{Å}$, and $c = 24.64\text{ }\text{Å}$, which correspond to the orthorhombic $\sqrt{2} \times \sqrt{2}$ distortion of the body-centered-tetragonal structure. No traces of other phases could be detected. The rocking curves have a full width at half maximum of 0.1° ,⁷ which is

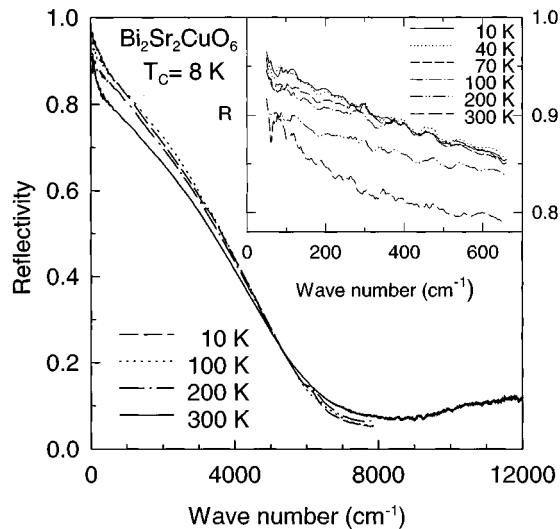


FIG. 1. Reflectivity of a $\text{Bi}_2\text{Sr}_2\text{CuO}_6$ single crystal at normal incidence and with the electric-field vector parallel to the ab plane for $T=10, 100, 200,$ and 300 K. Inset: reflectivity on an expanded scale for $T=10, 40, 70, 100, 200,$ and 300 K.

the minimum value so far reported. Both from the resistivity and the ac susceptibility we obtained the same values for the superconducting transition temperature ($T_c=7-8$ K) and for the transition width ($\Delta T_c=2$ K). Unlike earlier reports where a linear resistivity was observed down to the superconducting phase transition,^{8,9} in the present crystals $\rho(T)$ is only linear at high temperatures but saturates below 40 K (Ref. 10) at a residual resistivity with a sample to sample variation from 150 to 300 $\mu\Omega$ cm.

The reflectance measurements were made on the a - b plane of $\text{Bi}_2\text{Sr}_2\text{CuO}_6$ single crystals at normal incidence for temperatures from 300 K down to 10 K. We used two Fourier-transform spectrometers to cover the frequency range from 50 cm^{-1} to 12 000 cm^{-1} and a flow cryostat for the temperature variation. Absolute reflectivities were obtained by referencing the reflected intensity of the sample to a Au mirror with the same shape and size at each temperature. The systematic errors introduced due to the sample-reference interchange fell within 0.5%. A further confirmation of the absolute accuracy reached with this procedure comes from the small ($\approx 1\%$) mismatch in the absolute reflectivity in the overlap region between the FIR and MIR regions.

The temperature dependence of the reflectivity is shown in Fig. 1. Decreasing the temperature from 300 K down to 100 K the reflectivity shows an increase up to midinfrared frequencies. From 100 K down to 40 K the only increase in reflectivity occurs in the far-infrared range. The reflectivity is temperature independent below 40 K. The near-infrared reflectivity has a broad plasma minimum around 8700 cm^{-1} . Weak reproducible structure is observed at 181, 327, 427, and 508 cm^{-1} . The minima at 327 and 427 cm^{-1} coincide with the frequencies of the c -axis LO phonon modes of $\text{Bi}_2\text{Sr}_2\text{CuO}_6$.¹¹ Under ideal conditions (large perfect crystals with flat surfaces, perfectly s -polarized plane waves) leakage of c -axis longitudinal optical phonons into the ab -plane response can be excluded,¹² but some weak and surface-dependent leakage may occur if the experimental conditions

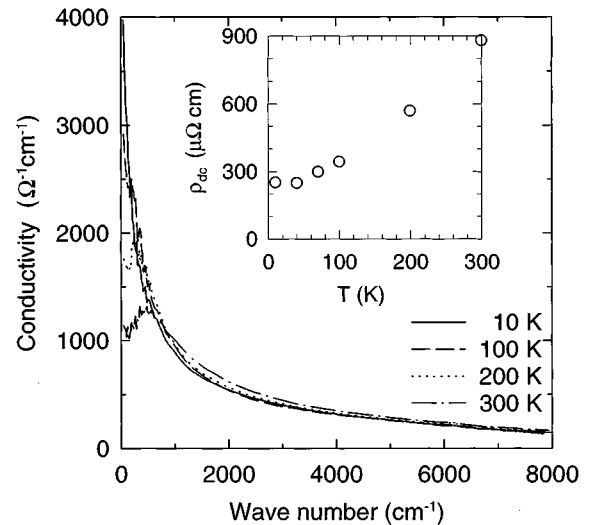


FIG. 2. Optical conductivity $\sigma(\omega)$ as a function of frequency for the same temperatures as in Fig. 1. Inset: dc resistivity obtained by extrapolating the optical conductivity to zero frequency.

are less than perfect. As the minima at 181 and 508 cm^{-1} are not seen for $\vec{E}\parallel c$, we attribute these to in-plane optical phonons.

To calculate the infrared conductivity through a Kramers-Kronig transformation we used a Hagen-Rubens extrapolation for the low-frequency region. Extrapolation towards high frequencies (up to 320 000 cm^{-1}) was done using the data of Terasaki *et al.*¹³

The real part of the conductivity σ_1 is shown up to 8000 cm^{-1} in Fig. 2 and in more detail up to 2000 cm^{-1} in Fig. 3. The conductivity at low temperatures is almost featureless and decreases monotonically with frequency. When the temperature is increased to 100 K, a maximum in the conductivity appears, which shifts to 500 cm^{-1} at room temperature. We also notice from the way the conductivity curves cross

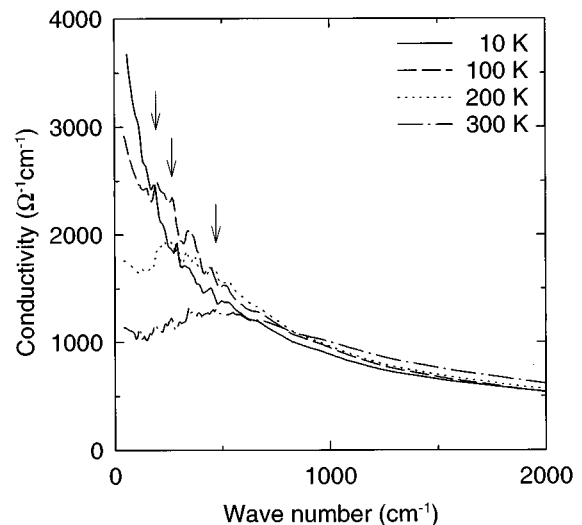


FIG. 3. Optical conductivity $\sigma(\omega)$ on an expanded scale for 10, 100, 200, and 300 K. The arrows indicate the evolution of the maximum.

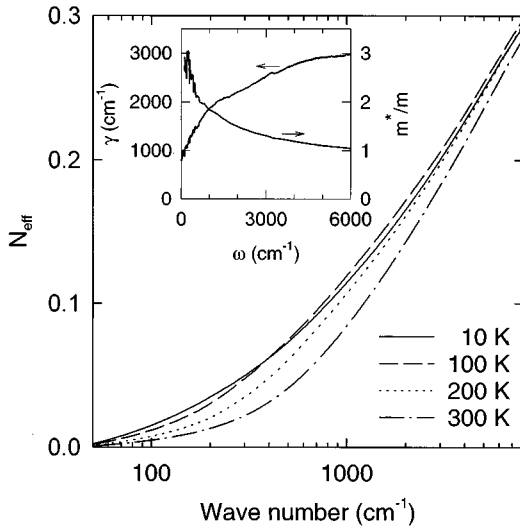


FIG. 4. Effective number of carriers per unit of CuO_2 calculated from $\sigma(\omega)$ using the partial f sum rule. Inset: frequency-dependent scattering rate [$\gamma(\omega)$] and effective mass enhancement [$m^*(\omega)/m$] at 10 K.

that at least part of the spectral weight removed from the low-frequency side of the spectrum is recovered in the mid-infrared range. To demonstrate this, we present in Fig. 4 the carrier density obtained from integrating $\sigma(\omega)$ up to a cutoff frequency [$n_{\text{eff}}(\omega_c) = 2m\pi^{-1}e^{-2}\int_0^{\omega_c}\sigma(\omega')d\omega'$]. The dc resistivity obtained by extrapolation of the optical conductivity to zero frequency is presented in the inset of Fig. 2. This shows a linear temperature dependence, which saturates below 40 K.

The fact that the single-layer compounds have almost the same volume per unit cell as the double- and triple-layer compounds results in a low free carrier concentration and a relatively low conductivity. Thus, one might expect that the contribution of low-frequency excitations, in particular optical phonons, can no longer be neglected. However, by applying the f sum rule [$\int_0^\infty 8\sigma_{\text{ion}}(\omega)d\omega = \sum_j 4\pi n_j Z_j^2/m_j$] to all ions with mass m_j and ionic charges Z_j , we calculate an average value of the conductivity due to phonons of only $18 \Omega^{-1} \text{cm}^{-1}$ in the range of 0–700 cm^{-1} , i.e., one order of magnitude smaller than the rise in conductivity between 0 and 500 cm^{-1} in Fig. 2. Hence the phonon contributions are far too weak to be the main source of this rise in conductivity.

The maximum near 500 cm^{-1} (indicated with arrows in Fig. 3) shifts to a lower frequency upon reducing the temperature, and is superimposed on a steeply falling free-electron conductivity which increases as the temperature is decreased. At 10 K the free-electron response is prevalent in the low-frequency conductivity. In the remainder of this paper we will indicate the depression of the conductivity below the maximum as a pseudogap. In the present case there is no unambiguous—and physically meaningful—way to decompose the conductivity in free-carrier and bound-charge components. One of the reasons is, that in the high- T_c cuprates also the intraband conductivity deviates considerably from standard Drude behavior. In particular the high- T_c cuprates, if optimally doped, are known to have a linear frequency

dependence of the scattering rate, as follows from inversion of the real and imaginary parts of $\sigma(\omega)$ using the expression¹⁴ $\sigma(\omega) = ne^2m^{-1}/\{\gamma(\omega) - i\omega m^*(\omega)/m\}$, where n is the carrier density, m is the band mass, $m^*(\omega)/m$ is the effective mass enhancement, and $1/\gamma(\omega)$ is the effective relaxation time. A further complication arises, if two or more electronic bands cross the Fermi level. In this case, which we believe to be relevant for $\text{Bi}_2\text{Sr}_2\text{CuO}_6$, the spectrum of $\sigma(\omega)$ contains interband transitions in addition to the intraband components. The interband part has a complex line shape which depends on the details of the band dispersion and the k -dependent optical transition matrix elements. Obviously if the material has two or more bands of electrons, at least one of which (the CuO_2 bands) has a frequency-dependent scattering rate, it is no longer possible to make a meaningful separation in several components. At low temperatures, where the CuO_2 channel has a reduced scattering rate, $\sigma(\omega)$ is dominated by the CuO_2 channel at least at the low frequencies. In this region one might hope to extract the frequency-dependent scattering rate of the CuO_2 carriers, at least up to a frequency where other contributions to $\sigma(\omega)$ become significant. For this reason we display in the inset of Fig. 4 the frequency-dependent scattering rate only for the lowest temperature. We notice that the linear behavior of $\gamma(\omega)$, which is rather typical for all high- T_c cuprates, exists only up to 0.1 eV in this case. In view of the possibility of low-energy interband transitions in this compound, even at 10 K $\gamma(\omega)$ extracted from optical data is probably no longer meaningful for $\hbar\omega > 0.1$ eV. Our observations support the conclusion by Romero *et al.*, based on an analysis of infrared transmission data, that the linear frequency dependence of $\gamma(\omega)$ is limited to the energy range below 0.1 eV.¹⁵ The nonlinear temperature dependence of the resistivity in the crystals used for this study is also inconsistent with MFL behavior at the lowest temperatures.

Transmission experiments on free-standing nonsuperconducting single crystals of $\text{Bi}_2\text{Sr}_2\text{CuO}_6$ performed by Romero *et al.*¹⁵ also reveal a singularity in the FIR conductivity, although the effect is less pronounced. The room-temperature conductivity shows a clear change of slope around 500 cm^{-1} , and the frequency-dependent effective mass $m^*(\omega)$ has a minimum at this frequency. While only a trace of the pseudogap is observed in nonsuperconducting single crystals,¹⁵ the effective number of carriers remains the same. A maximum in the optical conductivity was also observed in the related single-layer compound $\text{Tl}_2\text{Ba}_2\text{CuO}_6$,¹⁶ although a substantially larger spectral weight was involved.

A possible candidate for the observed pseudogap is the additional electronic degree of freedom introduced by having both hole-doped CuO_2 and electron-doped BiO bands. Although an interpretation in terms of direct transitions between these bands is probably too simple due to the strong electron-electron correlations in the Cu-O bands, a pseudogap may nevertheless exist, not unlike the situation encountered in Kondo insulators.¹⁷ The LAPW band calculations of Singh and Pickett² give two types of bands: For a vanishing orthorhombic distortion there is a large Cu-O-derived barrel section centered at X and its $\sqrt{2} \times \sqrt{2}$ -folded counterpart centered around Γ . In addition there are two Bi-O-derived electron pockets with their Brillouin-zone-folded

counterparts, all of them centered at \bar{M} . As suggested by Singh and Pickett,² a weak structural change from tetragonal to orthorhombic strongly affects the structure of the electronic bands. The bands are shifted up to 400 meV for Bi displacements of 0.14 Å and 0.41 Å for O. As a result five bands were calculated for k close to the saddle point (\bar{M}), all within a range of 200 meV around E_F . Only two of the Bi-O pockets (one of them barely) cross E_F when the orthorhombic distortions are taken into account. Because the band structure is strongly affected by modulations of the lattice, it can also have an appreciable temperature dependence. Photoemission studies have revealed a single occupied band near E_F close to the \bar{M} point, which was originally indicated as a possible BiO-derived band¹⁸ but was identified as a CuO₂ band in a later publication.¹⁹ The absence of a clear BiO-derived band in photoemission may, however, result from a disorder-induced smearing of the k dispersion in the BiO layers, or from the small photoelectron cross section for Bi and O states compared to the Cu 3d cross section. The main “generalized Drude” component in our data then originates from the CuO barrels, with a linearly frequency-dependent decay rate typical for optimally doped cuprates. The pseudogap at high temperatures would be due to transitions between the closely spaced bands which cross E_F near \bar{M} . In this scenario the disappearance of the pseudogap at low temperatures can reflect a gradual change of atomic coordinates upon cooling, with a corresponding change of the interband separation.

This structural modulation can easily result in a redistribution of carriers between BiO and CuO₂ bands and the disappearance of the pseudogap. Interestingly, large lattice distortions are generally present in films, which show a higher T_c and a more pronounced pseudogap.²⁰

We have presented experimental data on the in-plane infrared response of superconducting Bi2201 single crystals for temperatures from 10 K to 300 K. The optical conductivity shows a pseudogap feature that shifts with temperature. The optical conductivity is at least one order of magnitude too large to be compatible with a purely phononic interpretation of this feature. This observation indicates the presence of two coupled conducting channels and may provide important clues regarding the fact that T_c in the single-layer Bi cuprate material is much lower than in other nearly stoichiometric compounds. We discuss the possibility that the pseudogap is related to electronic transitions between bands near the \bar{M} point, which are strongly coupled to the orthorhombic lattice distortion.

We gratefully acknowledge many useful comments from W. N. Hardy. This investigation was supported by the program for Russian-Dutch Cooperation under Project No. 047003033 of the Nederlandse Organisatie voor Wetenschappelijk Onderzoek, the Russian Scientific Technical Program “High Temperature Superconductivity” (A.A.T., J.I.G., and G.A.K.), and the program Human Capital and Mobility under Contract No. ERBCHBICT941820 (J.S.).

-
- ¹G. Jehl *et al.*, Europhys. Lett. **17**, 255 (1992).
²D. J. Singh and W. E. Pickett, Phys. Rev. B **51**, 3128 (1995).
³C. M. Varma *et al.*, Phys. Rev. Lett. **26**, 1996 (1989).
⁴P. W. Anderson, Phys. Rev. Lett. **67**, 2092 (1991).
⁵S. V. Shulga *et al.*, Physica C **178**, 226 (1991).
⁶J. I. Gorina *et al.*, Solid State Commun. **91**, 615 (1994).
⁷V. P. Martovitsky *et al.*, Solid State Commun. **96**, 893 (1995).
⁸S. Martin *et al.*, Phys. Rev. B **41**, 846 (1990).
⁹X. H. Hou *et al.*, Phys. Rev. B **50**, 496 (1994).
¹⁰S. I. Vedenev *et al.*, Phys. Rev. B **51**, 16 380 (1995).
¹¹A. A. Tsvetkov, J. Schützmann, and D. van der Marel (unpublished).
¹²D. van der Marel *et al.*, Phys Rev. Lett. **71**, 2676 (1993).
¹³I. Terasaki *et al.*, Phys. Rev. B **41**, 865 (1990).
¹⁴J. W. Allen and J. C. Mikkelsen, Phys. Rev. B **15**, 2952 (1977).
¹⁵D. B. Romero *et al.*, Solid State Commun. **82**, 183 (1992).
¹⁶A. V. Puchkov *et al.*, Phys. Rev. B **51**, 3312 (1995).
¹⁷G. Aeppli and Z. Fisk, Comments Condens. Matter Phys. **16**, 155 (1992).
¹⁸E. R. Ratner *et al.*, Phys. Rev. B **48**, 10 482 (1993).
¹⁹D. M. King *et al.*, Phys. Rev. Lett. **73**, 3298 (1994).
²⁰P. Calvani *et al.*, Phys. Rev. B **53**, 2756 (1996).